JOURNAL OF THERMOPHYSICS AND HEAT TRANSFER
Vol. 10, No. 3, July–September 1996

Radiative Properties of Fibrous Insulations: Theory Versus Experiment

G. R. Cunnington* and S. C. Lee†
Applied Sciences Laboratory, Inc., Hacienda Heights, California 91745

The validity of an exact theoretical model for calculation of the radiative properties of high-porosity, randomly oriented fiber media is examined by comparing experimental measurements with theoretical predictions for spectral reflectance and transmittance. Spectral hemispherical reflectances and spectral normal transmittances were calculated at wavelengths from 1.5 to 10.0 μm for several thicknesses of three types of thermal insulating materials having randomly oriented silica fibers of different size distributions. Theoretical results are compared with experimental measurements made on each of the three materials. The theoretical methodology, analytical results, and experimental characterizations of geometric parameters and radiative properties of the test materials are presented. The comparison shown between theory and experiment is excellent. Thus, the model is considered to be a valid tool for prediction of radiative properties of high-porosity, randomly oriented fibrous media.

Nomenclature

d^2F = fiber orientation distribution function
F_v = fiber volume fraction
I = intensity
$i(\eta, \phi)$ = isolated fiber scattering intensity distribution
K_e = extinction coefficient
L = thickness
N = number of fiber sizes
p = phase function
Q = single fiber efficiency
R = reflectance
r = fiber radius
T = transmittance
x_i = fractional volume of fibers of radius r_i
η = included angle between incident and scattered directions
θ = single fiber scattering observation angle
μ = direction cosine of angle ξ
ξ = azimuthal angle of incidence direction
σ_s = scattering efficiency
ϕ = angle of scattered intensity
Ω = solid angle
ω = polar angle of incidence direction

Subscripts
e = extinction
f = fiber
s = scattering
λ = wavelength

Superscript
$'$ = directional value

Introduction

ANALYSIS of radiative transfer through a scattering and absorbing medium requires the solution of the radiative transfer equation (RTE). The extinction, absorption, and scattering coefficients and the scattering phase function are the fundamental parameters required by the RTE. The accurate prediction of these radiative properties, which are governed by the geometric and optical properties of the scatterers, is necessary to obtain an accurate solution for radiative transfer. Fibrous thermal insulations are typically a high-porosity, dispersed medium. In this case, the average spacing between scatterers is much greater than their diameter and the wavelength of the incident radiation, so that the scatterers behave as isolated cylinders and independent scattering may be assumed.

Thermal radiative energy transport through fibrous insulations has received considerable attention in recent years. Earlier studies[1–7] addressed the problem of energy transport in high-porosity commercial insulations from cryogenic to very high temperatures. Radiation heat transfer analyses included approximate models that assume randomly oriented fibers[8,9] and more rigorous models that account for the morphology of the medium.[10–13] In particular, formulations for the effective properties of the medium, which include the extinction, absorption, and scattering coefficients and the scattering phase function, have been developed for arbitrary fiber orientations.[10–13] These radiative properties have been applied by Jeandel et al.[14] to investigate radiative transfer through a layer of silica fibers randomly oriented in planes.

A recent literature review[15] indicates that the radiative properties can be obtained either by applying analytical models that account for the morphology of the medium or from an inverse determination based upon experimental data. The models of Lee[10–13] belong to the former approach, whereas the latter approach involves the empirical fitting of the solution of the RTE with measured data such as hemispherical and/or directional reflectance and transmittance.[16–18] The extinction coefficient, scattering albedo, and the scattering phase function are handled parametrically in the solution of the RTE. An isotropic or anisotropic phase function such as the Henyey–Greenstein model with an asymmetry factor is usually assumed. This method typically involves the determination of a large number of variables from the empirical fitting. For example, the inverse determination by Nicolau et al.[19] involves six parameters. A deficiency of this method is that the uniqueness of the fitted parameters is questionable, and these properties have no correspondence with the true physical characteristics of the scattering medium. One important application of the inverse method is the determination of the effective refractive index

Presented as Paper 95-2023 at the AIAA 29th Thermophysics Conference, San Diego, CA, June 19–22, 1995; received Sept. 1, 1995; revision received Jan. 25, 1996; accepted for publication Jan. 30, 1996.

*Consultant; currently at Cunnington Associates, Palo Alto, CA 94306.
†Vice President. Senior Member AIAA.

of fibrous or particulate materials.[20,21] This effective index accurately reflects the real property for the specific material morphology, structure, and composition.

The theoretical formalisms of Lee,[10-13] once validated with experimental data, offer great utility for analysis and optimization of high-porosity fibrous media for a broad range of materials and fiber size distributions. The comparisons of the theory and experimental data for three well-characterized silica fiber insulations are presented in this article for the purpose of testing the validity of the theoretical models.

Theory

Thermal insulations are typically composed of fibers a few millimeters in length and several micrometers in diameter. They are commonly modeled as infinitely long circular cylinders as the fiber length is much greater than the fiber diameter and the wavelength of the incident radiation. Because an infinite cylinder behaves as a two-dimensional particle, the scattered radiation propagates along the surface of a cone with an apex angle equal to $\pi - 2\phi$, where ϕ is measured from the normal to the fiber axis. The radiative properties, which include the extinction, absorption, and scattering efficiencies, and the scattering intensity distribution, are given in terms of expansion coefficients that are a function of the fiber diameter, complex index of refraction, and wavelength. The basic formulas may be found in the literature, such as Kerker,[22] and will not be repeated herein.

To obtain the radiative properties of high-porosity fibrous media, the orientation and size distribution of fibers must be considered. The formulation that rigorously accounts for both of these effects has been developed by Lee.[10-13] The radiative properties models are summarized as

$$\{K_{e\lambda},\ \sigma_{s\lambda}\} = \int_{\omega_{f1}}^{\omega_{f2}} \int_{\xi_{f1}}^{\xi_{f2}} \int_{r_1}^{r_2} 2r\{Q_{e\lambda},\ Q_{s\lambda}\}N(r)\ \mathrm{d}r\mathrm{d}^2F \qquad (1)$$

The difference between the extinction and scattering coefficients gives the absorption coefficient. In Eq. (1), $(\omega_{f2},\ \omega_{f2})$ and $(\xi_{f1},\ \xi_{f2})$ denote the range of the polar and azimuthal orientations of d^2F. In general, these radiative coefficients vary with the incident direction, except for the special case of fibers randomly oriented in space. Because the scattering cross section of a fiber varies with the incidence angle, the product of scattering coefficient and scattering phase function p_λ must be considered as a group. This product is given by

$$\sigma_{s\lambda}p_\lambda(\xi,\ \omega,\ \eta) = \frac{4\lambda}{\pi^2}\int_{\omega_{f1}}^{\omega_{f2}} \int_{\xi_{f1}}^{\xi_{f2}} \int_{r_1}^{r_2} \frac{i(\eta,\ \phi)}{\sin\theta\cos^2\phi}N(r)\ \mathrm{d}r\mathrm{d}^2F \qquad (2)$$

where η is given by

$$\cos\eta = \mu\mu' + [(1-\mu^2)(1-\mu'^2)]^{1/2}\cos(\omega - \omega') \qquad (3)$$

In the present study test data on Space Shuttle tile materials are used for comparison with the theory. These thermal protection materials are a high-porosity fibrous medium that contain specific size distributions of fibers randomly oriented in space. The formulas for the radiative properties of these materials follow from Eqs. (1) and (2) as

$$K_{e\lambda} = \frac{2F_v}{\pi}\sum_{i=1}^{N}\frac{x_i}{r_i}\int_0^{2\pi} Q_{e\lambda}(\eta,\ \phi)\cos\phi\ \mathrm{d}\phi \qquad (4)$$

$$\sigma_{s\lambda} = \frac{2F_v}{\pi}\sum_{i=1}^{N}\frac{x_i}{r_i}\int_0^{2\pi} Q_{s\lambda}(r_i,\ \phi)\cos\phi\ \mathrm{d}\phi \qquad (5)$$

$$\sigma_{s\lambda}p(\eta) = \frac{4F_v\lambda}{\pi^4}\sum_{i=1}^{N}\frac{x_i}{r_i^2}\int_0^{\pi/2}\frac{i(\eta,\ \phi)}{\sin\theta\cos\phi}\mathrm{d}\phi \qquad (6)$$

The experimental data used to validate the theoretical model are spectral hemispherical reflectance and spectral normal transmittance of planar slabs of material samples illuminated with collimated irradiation at normal incidence. These quantities are predicted by solving the RTE

$$\mu\frac{\mathrm{d}|_\lambda}{\mathrm{d}y} + K_{e\lambda}|_\lambda = \frac{1}{4\pi}\int_{4\pi}\sigma_{s\lambda}p_\lambda(\eta)|_\lambda(\mu')\ \mathrm{d}\Omega' \qquad (7)$$

for collimated incidence utilizing the radiative properties of Eqs. (4-6). Emission is neglected because the material is at room temperature. The boundary condition for incident intensity I_0 is

$$I_\lambda(y = 0) = I_0\delta(\omega)\ \mathrm{d}(\mu - 1) \qquad (8)$$

The RTE is solved by the method of discrete ordinates utilizing a 40-point Gaussian quadrature. Details of this solution method can be found in texts on radiation, such as Brewster.[23] The angular distributions of the transmitted and reflected intensities are obtained. The hemispherical reflectance is given by

$$R_\lambda = \pi\int_{-1}^{0} I_\lambda(\mu,\ y = 0)\mu\frac{\mathrm{d}\mu}{I_0} \qquad (9)$$

and the normal transmittance is

$$T_\lambda = \pi\int_{\Delta\Omega} I_\lambda(\mu,\ y = L)\frac{\mathrm{d}\Omega}{I_0} \qquad (10)$$

where $\Delta\Omega$ is the solid angle subtended by the detector.

Prediction of fiber radiative properties requires the accurate knowledge of the spectrally dependent effective complex index of refraction of the fibers as well as the fiber size distribution. The radiative properties, computed according to Eqs. (4-6), are then utilized in the RTE that is solved by the method of discrete ordinates. Typically, a 40-point Gaussian quadrature was used for the summation. Several cases were tested using a 96-point quadrature, and the difference in results between 40-96 points was insignificant.

Experimental Procedures

The experimental requirements for validation of the theory include the accurate characterization of the materials and a measurement technique for radiative properties that corresponds to the one-dimensional assumption of the model, i.e., a planar slab of the medium of finite thickness, but infinite in the in-plane dimensions. Characterization of the test materials includes fiber size distribution, fiber orientation, fiber diameter-to-length ratio, surface quality of fibers, fiber volume fraction, and complex refractive of the fiber material. For the reflectance and transmittance measurements the ratio of the diameter of the illuminated area to the thickness of a specimen was 10 or greater in all cases, to be consistent with the one-dimensional condition of the analytical model.

Test Specimens

For this study, the test materials are a bonded silica fiber rigid insulation that is used for the thermal protection tiles of the Space Shuttle Orbiter. The designation of the material is LI900. It has a typical bulk density of 145 kg/m^3 that corresponds to a fiber volume fraction of nominally 0.066. This material had been produced from fibers of three different size distributions during its evolution from 1973 to the present. Also, two sources of raw silica fibers were used during the initial development phase. The choice of this family of insulations was based on the availability of spectral reflectance and transmittance data and accurate fiber size distribution characterizations for each of the three fiber type and size variables. Additional considerations were the rigid nature of the material

that permitted preparation of test specimens of accurate and uniform thickness, and the use of high-purity fibers so that the initial choice of complex refractive index for the theoretical calculations could be that of fused silica.[24] Fiber bonding is done with a colloidal silica that preserves the chemical purity of the system.

Fiber size distributions, measured using scanning electron microscopy (SEM) for the three types of materials, are shown in Fig. 1. The number of individual fibers counted for each case was typically 100. The letters A and B in the fiber-type designation denote the two sources of raw fiber. The B2.3-type designation is for a recent production run, and the A1 and B2 materials are from earlier lots (1973 and 1974, respectively). Figure 2 shows a typical SEM photograph of the fiber matrix illustrating the physical size and geometric arrangement of the fibers. The surfaces of the fibers are relatively smooth and the fiber length-to-diameter ratio is large, which is consistent with the model assumption of an infinite cylinder. As seen in Fig. 2, there is a small departure from the truly random fiber orientation assumption. In the plane of this figure the horizontal direction is the in-plane direction of a specimen and the vertical corresponds to the through-the-thickness direction.

Test specimens were 2.54-cm-diam disks with thicknesses ranging from 0.10 to 0.30 cm. Each specimen was dimensioned and weighed to obtain the fiber volume fraction. The maximum uncertainties in F_v and thickness for the test specimens are 6.5 and 4.5%, respectively. Specimens were prepared in both the through-the-thickness (TT) direction, which is also the pressing direction in the casting process, and in the in-plane (IP) direction to evaluate any effect of the small degree of preferential fiber orientation on the radiative properties of the medium.

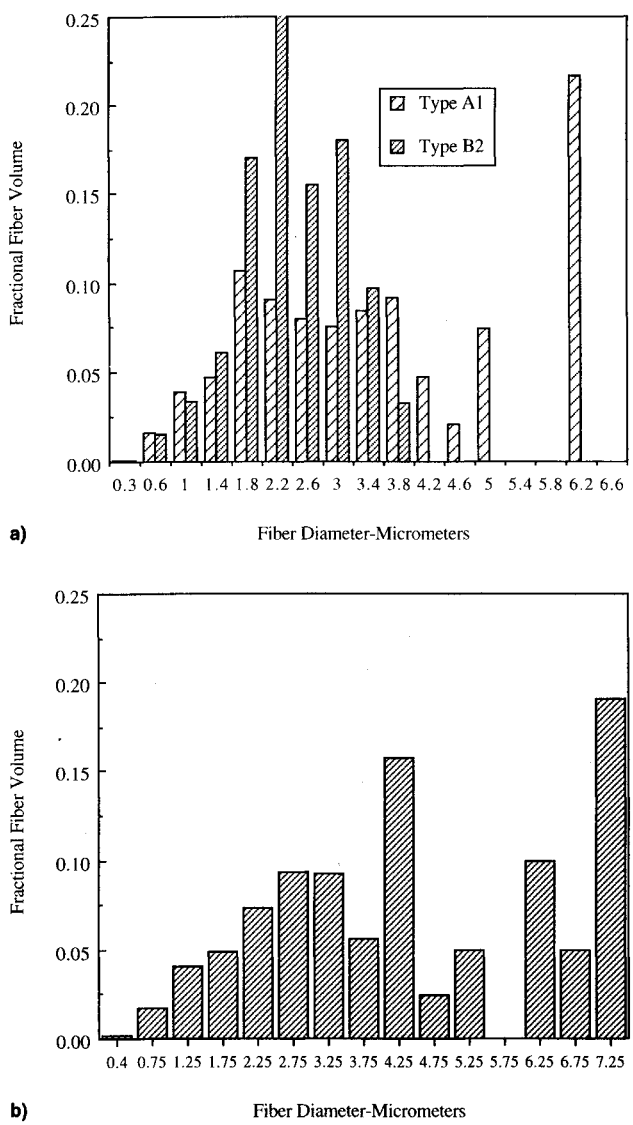

Fig. 1 Fiber size distributions for three types of fiber specimens: a) types A1 and B2 and b) type B2.3 fibers.

Experimental Apparatus

Spectral reflectance measurements were made over the wavelength interval of 1.5–10 μm using a Gier–Dunkle model HC-300 reflectometer.[25] The specimen is mounted on a water-cooled substrate having a diffuse reflectance of 0.040 or less over the wavelength interval of 1.5–10 μm. The specimen is illuminated hemispherically with uniform incident intensity. Reflected energy is collected from a 2.2-cm diameter specimen area in a 0.024-sr solid angle centered about a 7-deg angle with respect to a normal to the surface of the specimen. By reciprocity, the reflectance of a material irradiated at a given angle of incidence as measured by the energy collected over the total hemisphere of reflection is equal to the reflectance for uniform irradiation from the hemisphere as measured by the energy collected at a single angle of reflection. The reflected energy is passed through a prism monochromator to a detector whose output is measured with a lock-in amplifier. Reflectance is calculated from the ratio of detector signals when the specimen and the source are alternately viewed through the entrance slit of the monochromator. The estimated maximum uncertainty in reflectance amplitude is 0.005, and in wavelength it is 0.002 μm.

Spectral normal transmittance measurements were made by placing the specimen directly in front of the monochromator entrance slit. The specimen is illuminated at normal incidence by energy from a blackbody source. The source optical transfer system produces a slightly converging beam, a 2-deg cone half-angle, which has a diameter of 3.0 cm at the specimen position. Transmittance is calculated from the ratio of detector signals with and without the specimen placed over the entrance slit of the monochromator. Spectral resolution is the same as for the reflectance measurements, and the uncertainty in the transmittance value is 0.0002. For both reflectance and transmittance measurements at wavelengths greater than 3.5 μm, a short wavelength blocking filter is used in the monochromator to prevent stray energy, reflected within the monochromator

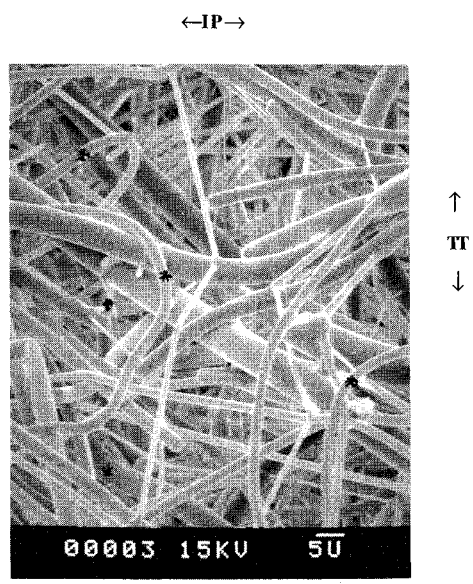

Fig. 2 SEM of typical fiber specimen, magnification = 1200×.

and not passing through the dispersive elements, from reaching the detector.

Results

Reflectance

Hemispherical spectral reflectance data for a specimen of the type B2.3 fiber material are shown in Fig. 3. The solid curve of the figure is the reflectance calculated using the theoretical model for the same value of the fiber volume fraction-thickness product F_vL as was measured for the test specimen (Fig. 1b). The initial calculation was performed using the literature values[24] of the refractive index of silica. Experimental reflectance data fall below the calculated values in the wavelength region between about 2.5–6.5 μm. An inversion technique was then used to derive effective refractive index values from the experimental results. These derived values, shown in Table 1, were then used for all subsequent analyses. The new correlations of numerical and experimental results are very good as discussed later in this section. The differences in absorption index from bulk material values are not unexpected. The influence of differences in surface morphology, structure, and composition is more pronounced for micrometer diameter fibers than for bulk material as the surface layer represents a much greater fraction of the total path length in the case of the fiber.

Table 1 Imaginary part of fiber refractive index k

Wavelength μm	k	
	Ref. 24	Derived
2.50	4.70e-6	3.29e-5
2.75	4.70e-6	2.90e-4
3.00	1.00e-5	2.00e-4
3.25	1.00e-5	1.50e-4
3.50	1.00e-5	1.00e-4
3.75	4.00e-5	1.35e-4
4.00	6.00e-5	1.74e-4
4.25	1.30e-4	3.05e-4
4.50	2.60e-4	5.20e-4
4.75	4.80e-4	1.50e-3
5.00	3.98e-3	3.98e-3
5.25	5.77e-3	6.00e-3
5.50	5.67e-3	9.07e-3
5.75	5.82e-3	9.12e-3
6.00	6.19e-3	9.16e-3
6.50	6.70e-3	9.38e-3

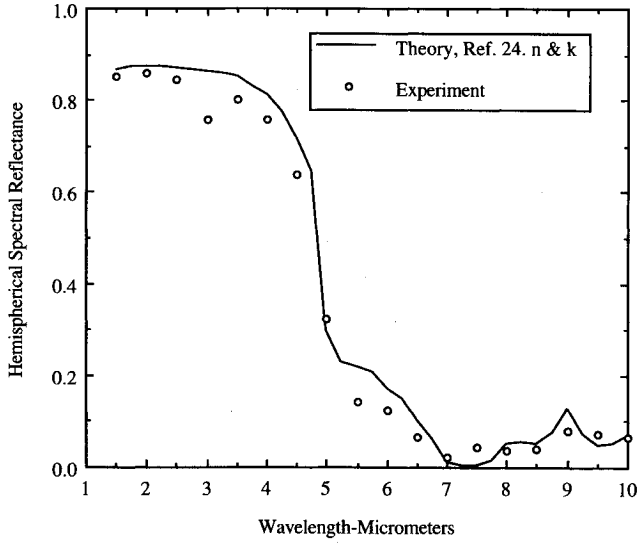

Fig. 3 Hemispherical spectral reflectance of type B2.3 fiber material, F_vL = 0.0102 cm.

Experimental data illustrating the effect of specimen orientation on reflectance are presented in Fig. 4. Test specimens of identical thickness were cut in two orthogonal directions in a block of type B2.3 fiber material. The thickness direction TT is the same as the pressing direction, and the IP direction is 90 deg to TT. The results show a lower reflectance for the IP direction that is consistent with the small degree of preferential fiber orientation seen in Fig. 2. Similar effects of specimen orientation are observed in the normal spectral transmittance data shown in Fig. 5. Higher transmittances are seen for the IP direction that are consistent with the lower reflectances seen in Fig. 4. The results of normal transmittance measurements made on eight duplicate pairs of types A1 and B2 fiber materials show the same orientation effects seen in Fig. 5. As this orientation effect is small for the test materials, no effort was made to model that variable.

Comparisons of the theoretical model predictions with experimental data for the hemispherical spectral reflectance of the type B2.3 fiber material for three F_vL values are shown by Fig. 6. The solid curves represent calculations made using the new values of the imaginary part of the complex refractive

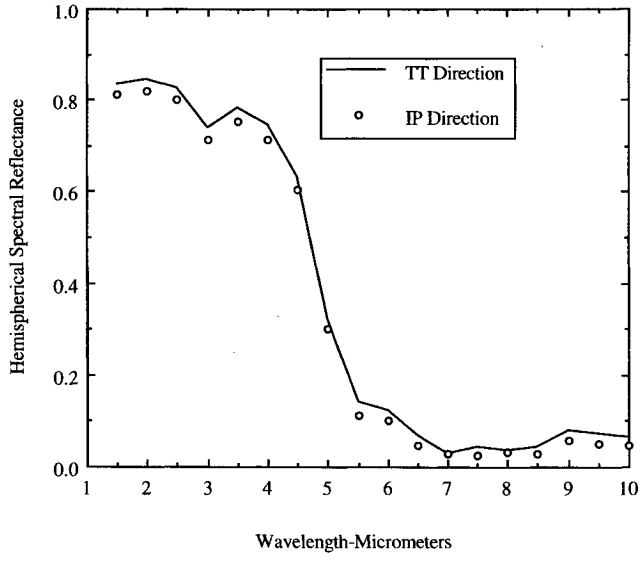

Fig. 4 Experimental hemispherical spectral reflectance data for B2.3 fiber material in TT and IP directions, F_vL = 0.0089 cm.

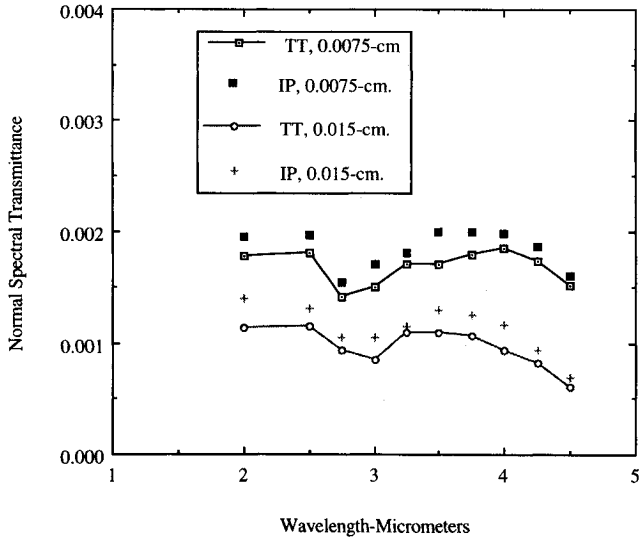

Fig. 5 Experimental normal spectral transmittance data for B2 fiber material in TT and IP directions, F_vL = 0.0075 and 0.015 cm.

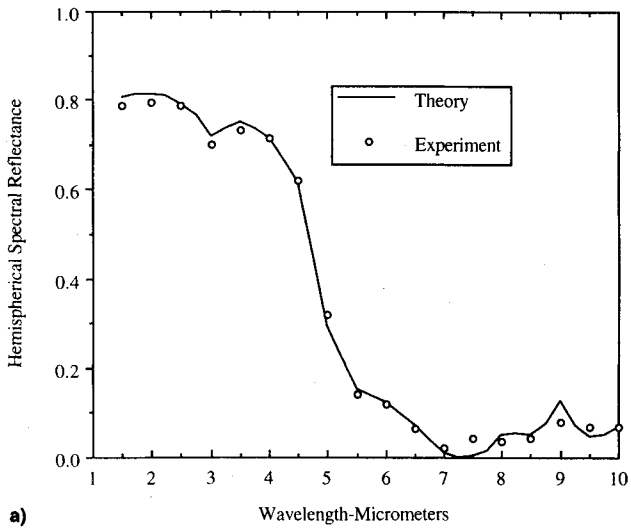

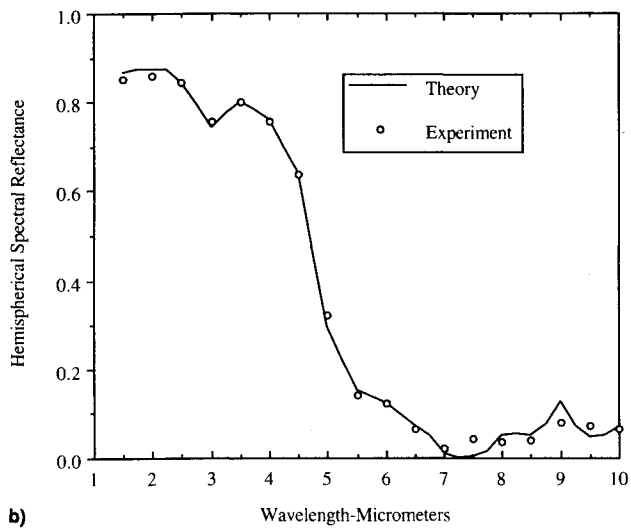

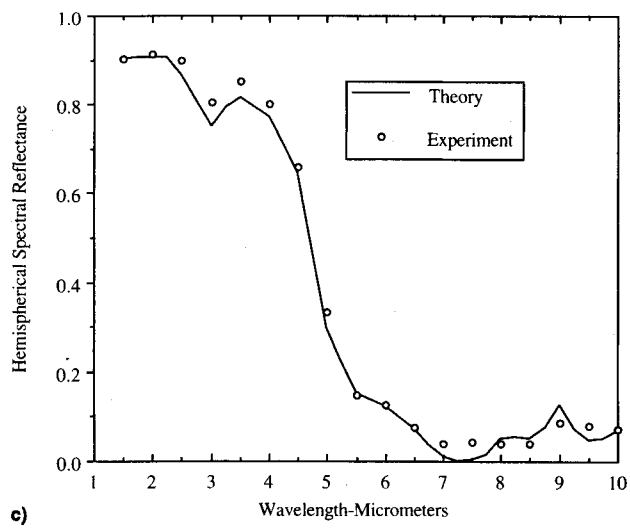

Fig. 6 Hemispherical spectral reflectance of type B2.3 material or three values of F_vL. F_vL = a) 0.0062, b) 0.0102, and c) 0.015 cm.

index as determined with the inversion technique using the experimental data of Fig. 3 for the F_vL = 0.0102-cm specimen. The agreement between experiment and theory for this case is shown in Fig. 6b. The agreement between predicted and experimental results for two additional cases of F_vL is seen in Figs. 6a and 6c.

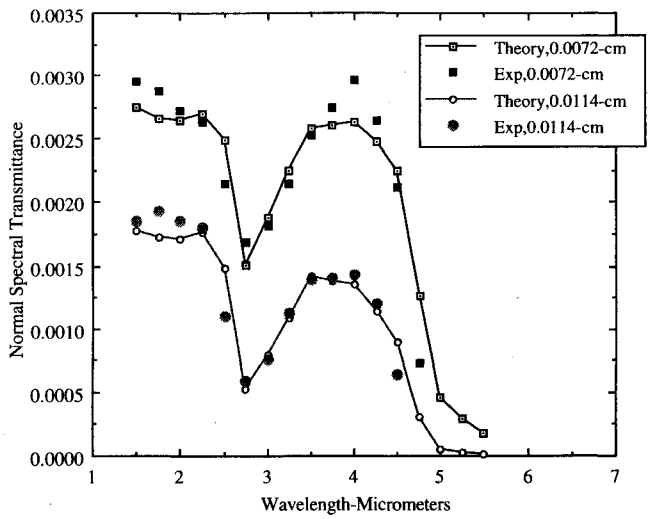

Fig. 7 Normal spectral transmittance of type B2.3 fiber material, F_vL = 0.0072 and 0.0114 cm.

Transmittance

Figure 7 shows the comparison between experimental data and theory for normal spectral transmittance of type B2.3 fiber material for two values of F_vL. The experimental data are generally in very good agreement with the predictions, considering that the maximum uncertainty in the transmittance measurement is 0.0002. The upper wavelength limitation of 4.75 μm for these experimental data is based upon the experimental uncertainty and the measured transmittances at longer wavelengths. Measured transmittances between 1.5–2.0 μm fall slightly above the calculation results. This may be the result of the slight preferential fiber orientation in the test materials as it effects scattering or the real part of the fiber refractive index. The theory predicts an albedo of unity in this wavelength region, and so absorption is not a consideration. No attempt was made to evaluate the sensitivity of the real part of the complex refractive index in this region.

Spectral normal transmittance data for two sets of type B2 fiber material are shown in Fig. 8 in comparison with the corresponding theoretical results. The strong normal transmittance between 6.75–7.5 μm is the result of the real part of the refractive of silica approaching unity at a wavelength of 7.25 μm, and scattering efficiencies become much smaller. The agreement between duplicate test specimens is very good at wavelengths of 6.5 μm and less, indicating a reasonably uniform spatial distribution of fiber volume fraction on a macroscopic level. However, because of the very large optical thicknesses in this wavelength region, the sensitivity to small differences in F_v is reduced. The specimen-to-specimen differences observed between 6.75–7.25 μm are more indicative of uniformity between specimens because of the smaller optical thickness over this wavelength interval.

The agreement between experiment and theory for the type A1 fiber materials is essentially the same as seen for the other materials. Figure 9 shows the comparison for two specimens, each at two values of F_vL. In the case of the type A1 fiber, we do not observe the absorption band between wavelengths of 2.5–3.5 μm that is seen for types B1 and B2.3 fibers. The calculations were repeated using the values of k from Ref. 24 for wavelengths from 1.5 to 4.0 μm, and those results are shown by the solid curves in the figures. The general agreement between theory and experiment is again very good. The type A fiber is from a different source than the type B fiber. The differences in effective refractive index and absorption may be attributed to structure–composition variations between the various fiber types. However, SEM and x-ray diffraction analyses show no obvious differences.

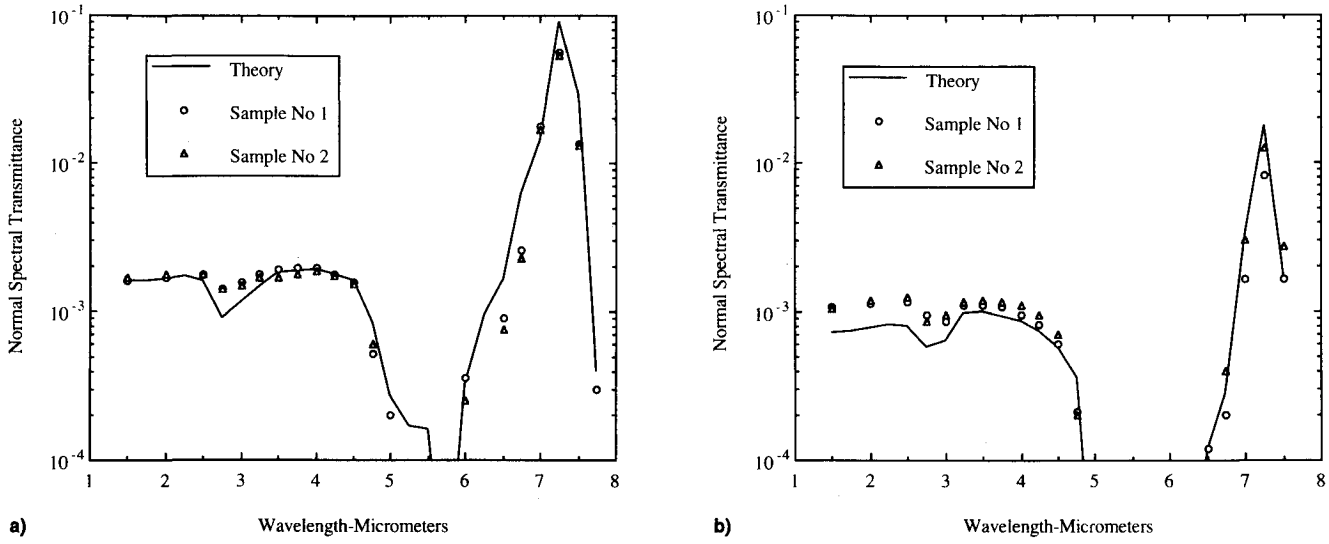

Fig. 8 Normal spectral transmittance of B2 fiber material. F_vL = a) 0.0072 and b) 0.015 cm.

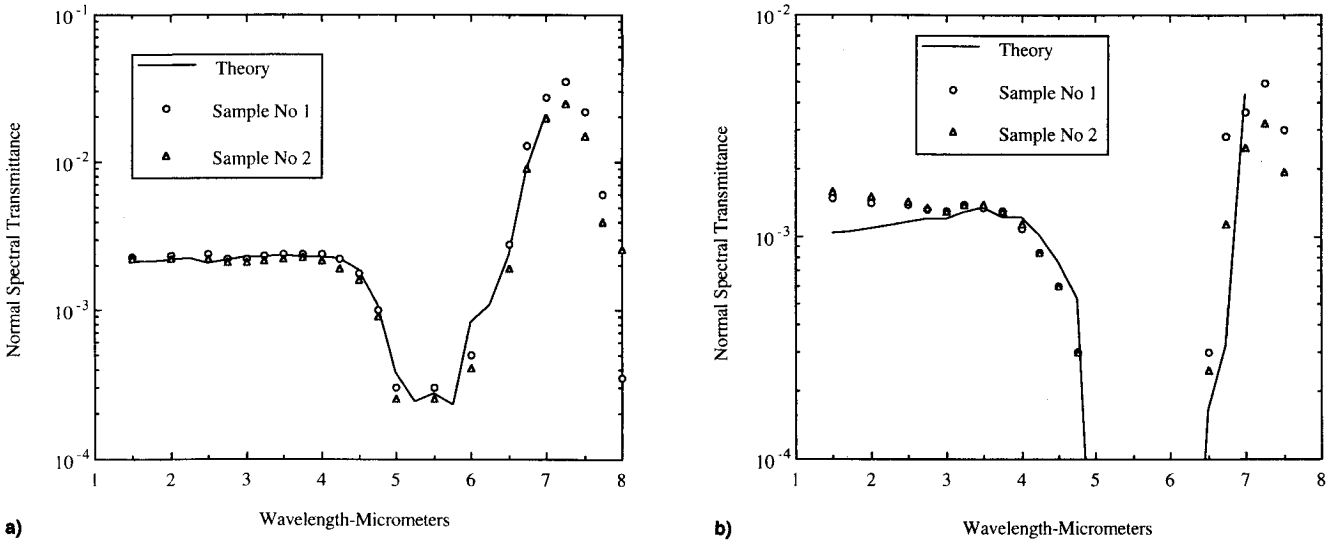

Fig. 9 Normal spectral transmittance of A1 fiber material. F_vL = a) 0.0072 and b) 0.015 cm.

Conclusions

The good agreement between theory and experimental data presented in this article demonstrate the validity of the theoretical formalisms of Lee[11-13] for the prediction of the radiative properties of high-porosity fibrous media having nearly random fiber orientation. The description of experimental data used for comparison with theoretical models must include a thorough characterization of the actual test materials, including size distribution, fiber morphology, and fiber composition and structure. Definition of a mean fiber size and a generic material description is not adequate for comparison with theory. As seen from this study, the absorption coefficient of the fibers may differ significantly from literature data for generic material. The inversion approach has been shown to be useful for determining the effective optical properties of the actual materials of the fibrous medium.

References

[1]Verschoor, J. D., and Greebler, P., "Heat Transfer by Gas Conduction and Radiation in Fibrous Insulation," *Transactions of the American Society of Mechanical Engineers*, Vol. 74, No. 6, 1952, pp. 961-968.

[2]Bankvall, C. G., "Heat Transfer in Fibrous Materials," *Journal of Testing and Evaluation*, Vol. 1, 1973, pp. 235-243.

[3]Larkin, B. K., and Churchill, S. W., "Heat Transfer by Radiation Through Porous Insulations," *Journal of the American Institute of Chemical Engineers*, Vol. 5, No. 4, 1959, pp. 467-474.

[4]Pelanne, C. M., "Heat Flow Principles in Thermal Insulations," *Journal of Thermal Insulation*, Vol. 4, 1980, pp. 27-44.

[5]Pettyjohn, R. R., "Thermal Conductivity Measurements on a Fibrous Insulation Material," *Proceedings of the 7th Conference on Thermal Conductivity*, National Bureau of Standards Special Publication 302, Gaithersburg, MD, Sept. 1968, pp. 729-736.

[6]Linford, R. M. F., Schmitt, R. J., and Hughes, T. A., "Radiative Contribution to the Thermal Conductivity of Fibrous Insulations," *Heat Transmission Measurements in Thermal Insulations*, American Society for Testing and Materials Special Publication 544, Philadelphia, PA, June 1974, pp. 68-84.

[7]Kagner, M. G., *Thermal Insulation in Cryogenic Insulation*, Israel Program for Scientific Translations, Cat. No. 2200, Jerusalem, 1965.

[8]Tong, T. W., and Tien, C. L., "Radiative Transfer in Fibrous Insulations—Part 1: Analytical Study," *Journal of Heat Transfer*, Vol. 105, 1983, pp. 70-75.

[9]Houston, R. L., and Korpela, S. A., "Heat Transfer Through Fiberglass Insulation," *Proceedings of the 7th International Heat Transfer Conference*, Vol. 2, Hemisphere, Washington, DC, 1982, pp. 499-504.

[10]Lee, S. C., "Radiation Heat Transfer Model for Fibers Oriented Parallel to Diffuse Boundaries," *Journal of Thermophysics and Heat Transfer*, Vol. 2, No. 4, 1988, pp. 303-308.

[11]Lee, S. C., "Effect of Fiber Orientation on Thermal Radiation in Fibrous Media," *International Journal of Heat and Mass Transfer*,

Vol. 32, No. 2, 1989, pp. 311–319.
[12]Lee, S. C., "Radiative Transfer Through a Fibrous Medium: Allowance for Fiber Orientation," *Journal of Quantitative Spectroscopy and Radiative Transfer*, Vol. 36, No. 3, 1986, pp. 253–263.
[13]Lee, S. C., "Scattering Phase Function for Fibrous Media," *International Journal of Heat and Mass Transfer*, Vol. 33, No. 10, 1990, pp. 2183–2190.
[14]Jeandel, G., Boulet, P., and Morlot, G., "Radiative Transfer Through a Medium of Silica Fibers Oriented in Parallel Planes," *International Journal of Heat and Mass Transfer*, Vol. 36, No. 3, 1993, pp. 531–536.
[15]Petrov, V. A., "Inverse Radiation Problems in Scattering Semitransparent Materials Based on the Radiation Diffusion Approximation," *Proceedings of the 13th European Conference on Thermophysical Properties*, Lisbon, Portugal, 1993.
[16]Yeh, H. Y., and Roux, J. A., "Spectral Radiative Properties of Fiberglass Insulations," *Journal of Thermophysics and Heat Transfer*, Vol. 1, No. 1, 1989, pp. 78–81.
[17]Kamiuto, K., Sato, M., and Iwamoto, M., "Determination of the Radiative Properties of High-Porosity Materials by Use of the Emerging-Intensity Fitting Method," *Journal of Quantitative Spectroscopy and Radiative Transfer*, Vol. 42, No. 4, 1989, pp. 477–482.
[18]Kuhn, J., Korder, S., Arduini-Schuster, M. C., Gobel, G., and Fricke, J., "Infrared-Optical Properties of Insulating Powders," *Proceedings of the 13th European Conference on Thermophysical Properties*, Lisbon, Portugal, 1993.
[19]Nicolau, V. P., Raynard, M., and Sacadura, J. F., "Spectral Radiative Properties Identification of Fiber Insulating Materials," *International Journal of Heat and Mass Transfer*, Vol. 37, Suppl. 1, 1994, pp. 311–324.
[20]Manickavasagam, S., and Menguc, M. P., "Effective Optical and Radiative Properties of Coal Particles as Determined from FT-IR Spectroscopy Experiments," *Energy and Fuel*, Vol. 7, No. 6, 1993, pp. 860–869.
[21]Menguc, M. P., Manickavasagam, S., and D'sa, D. A., "Determination of Radiative Properties of Pulverized Coal Particles from Experiments," *Fuel*, Vol. 73, No. 4, 1994, pp. 613–625.
[22]Kerker, M., *The Scattering of Light and Other Electromagnetic Radiation*, Academic, New York, 1969, Chap. 6.
[23]Brewster, M. Q., *Thermal Radiative Transfer and Properties*, Wiley, New York, 1992, Chap. 12.
[24]Palik, E. D., *Handbook of Optical Constants of Solids*, Academic, Orlando, FL, 1985.
[25]Dunkle, R. V., Edwards, D. K., Gier, J. T., Nelson, K. E., and Roddick, R. D., "Heated Cavity Reflectometer for Angular Reflectance Measurements," *Progress in International Research on Thermodynamic and Transport Properties*, Academic, New York, 1962.